Ad Hoc Networks 27 (2015) 68–80

Contents lists available at ScienceDirect

Ad Hoc Networks

journal homepage: www.elsevier.com/locate/adhoc

On the impact of interference models on channel assignment in multi-radio multi-channel wireless mesh networks

Aizaz U. Chaudhry *, Roshdy H.M. Hafez, John W. Chinneck

Department of Systems and Computer Engineering, Carleton University, Ottawa, Canada

ARTICLE INFO

Article history:
Received 12 July 2013
Received in revised form 23 October 2014
Accepted 27 November 2014
Available online 3 December 2014

Keywords:
Channel assignment
Multi-radio multi-channel
Wireless mesh networks

ABSTRACT

We study the impact of three different interference models on channel assignment in multi-radio multi-channel wireless mesh networks, namely the protocol model, the signal-to-interference ratio (SIR) model and the SIR model with shadowing. The main purpose is to determine the minimum number of non-overlapping frequency channels required to achieve interference-free communication among the mesh nodes based on a realistic interference model. We propose novel, effective, and computationally simple methods for building the conflict graph based on the SIR model with shadowing, and for finding channel assignments from the resulting conflict graph. We find that channel assignment using a realistic interference model (SIR model with shadowing) requires more frequency channels for network throughputs at different node-degree constraints as compared to using simpler interference models.

1. Introduction

The protocol model [1] is widely used to model interference for channel assignment in wireless mesh networks. This simple model assumes that interference is a binary phenomenon that occurs within the interference range of the nodes of any active link. The SINR (signal-to-interference-and-noise ratio) model, also known as the physical model [1], is more accurate. It considers the cumulative effect of interference at the receiving node where a packet is received correctly if its SINR is above a certain threshold, commonly known as the SINR threshold. Neither the protocol model nor the SINR model reflects the reality of signal propagation in wireless links. In a real wireless channel, the RF signal is reflected from and around nearby objects, which causes the signal strength to fluctuate in space. This effect is commonly known as *shadowing* and is usually accounted for by adding a random component to the received signal strength. An improved physical model that accounts for shadowing will be referred to as *SINR model with shadowing*. We use SIR (signal-to-interference ratio) instead of SINR since co-channel interference is generally much stronger than noise. Our goal is to use the realistic *SIR model with shadowing* to devise an interference-free channel assignment method for multi-radio multi-channel (MRMC) wireless mesh networks (WMNs).

To achieve our objective, we propose a novel and computationally simple method of building the conflict graph based on the SIR model, then extend it for the SIR model with shadowing. We also develop new computationally simple heuristics to find a small number of frequency channels for interference-free channel assignment by finding *weighted maximal independent sets* (WMaISs) in the conflict graph. Note that in these SIR models interference is controlled but still exists. By "interference-free" communication we mean that the incoming packet's SIR is above the required SIR threshold for correct reception at the receiver.

To minimize the number of frequency channels required, we use our *Select x for less than x* topology control algorithm (TCA) [2] for building the connectivity graph. We

* Corresponding author.
E-mail addresses: auhchaud@sce.carleton.ca (A.U. Chaudhry), hafez@sce.carleton.ca (R.H.M. Hafez), chinneck@sce.carleton.ca (J.W. Chinneck).

http://dx.doi.org/10.1016/j.adhoc.2014.11.019
1570-8705/

assume a single mesh gateway (GW), which is the sink for all flows. All mesh nodes, except the GW, are sources of flow that can take multiple paths to the GW. We formulate this multi-path routing problem as a mixed integer linear program whose objective is to maximize the network throughput while maintaining fairness among the multiple flows under flow conservation, half-duplex, and node-degree constraints. By *network throughput*, we mean the total amount of flow that reaches the GW from all sources. We formulate the interference-free channel assignment problem as a minimum coloring problem, known to be NP-hard for general graphs [3]. Given the conflict graph generated by the SIR model with shadowing, the minimum coloring problem requires finding the smallest number of WMaISs where the number of frequency channels required is equal to the number of WMaISs. Our results show that channel assignment using the SIR model with shadowing requires the highest number of frequency channels for network throughputs at different node-degree constraints as compared to using other interference models, due to its more realistic nature.

To the best of our knowledge, this is the first work to propose a method for finding a small number of frequency channels needed for interference-free communication in MRMC WMNs under realistic conditions. Related preliminary work has been presented in [4]. Our contributions include (i) the development of a simple and effective method for implementing a conflict graph based on the SIR model with shadowing, which significantly reduces the overall computational complexity, (ii) novel, computationally simple and effective heuristics for finding a small number of non-overlapping frequency channels for realistic interference-free channel assignment for MRMC WMNs, and (iii) showing that more realistic interference models require a significant increase in the number of frequency channels needed for interference-free communication.

The rest of the paper is organized as follows. Section 2 presents related work. Section 3 explains the creation of the conflict graph using three different interference models. The solution of the channel assignment problem using WMaISs is presented in Section 4. Performance evaluation with results is given in Section 5. Conclusions and some directions for future work are given in Section 6.

2. Related work

Several channel assignment schemes have been proposed which use the protocol model for modeling interference in MRMC WMNs [5–11] due to its simplicity and ease of implementation. However the study in [12] concludes that cumulative interference must be taken into account to obtain accurate performance results for multi-hop wireless networks and recommends the use of the cumulative interference model, i.e. SIR model. The study also states that although the physical model is necessary for accuracy, it is not suitable for large-scale multi-hop wireless networks due to its high computational complexity. We enhance the SIR model to include shadowing and use it in finding interference-free channel assignments using a minimum coloring heuristic that repeatedly solves the WMaIS sub-problem to determine a small number of frequency channels required. WMaISs have previously been used for resource allocation in multi-hop wireless networks, e.g. for link scheduling in MRMC multi-hop wireless networks [13] and in ultra wideband wireless ad-hoc networks [14]. Schemes using minimum coloring for resource allocation in wireless networks have also been proposed. The problem of determining the minimum number of frequency bands required for multi-radio multi-hop wireless networks such that all co-located transmitters and receivers can be simultaneously activated is addressed in [15]. Instead of using the link interference graph, a minimum coloring method is used to find a feasible spectrum allocation directly from the network connectivity graph. A simplistic interference model based on duplexing constraints in which a node is restricted from simultaneously transmitting and receiving on the same frequency band is used. In [16], the authors use minimum coloring for TDMA link scheduling in a multi-hop wireless network to maximize its throughput. They construct the conflict graph using the protocol interference model or the RTS/CTS interference model [17]. Minimum coloring for the link interference graph is used in [18] to solve the problem of obtaining tight delay guarantees for throughout-optimal link scheduling in wireless ad-hoc networks. A scheduling algorithm is proposed in [19] that uses minimum coloring to determine a minimum length schedule for maximizing the network throughput in TDMA based wireless mesh networks. The interference model used assumes that transmissions may interfere in two ways which are typically referred to as primary and secondary interference [20]. The authors assume that there are enough orthogonal channels available to eliminate all the secondary interference, i.e. the interference that arises between two links when the receiver of one link is within the interference range of the transmitter of the other link. They consider the primary interference only while constructing the link conflict graph in which the links conflict with each other if they share a common sender or receiver.

Unlike any previous channel assignment schemes for MRMC WMNs, our work is the first to propose a channel assignment method that is based on a realistic interference model, i.e. the SIR model with shadowing. Our method determines a channel assignment that provides interference-free communication among the mesh nodes in a MRMC WMN to achieve the maximum network throughput while maintaining fairness among the multiple network flows.

3. Interference models

The conflict graph F can be built using the three different interference models once the links involved in routing are known. The vertices in F correspond to the links in the connectivity graph C. An edge between vertices l_{ij} and l_{pq} in F indicates that the links l_{ij} and l_{pq} in C cannot be active simultaneously. Node locations are assumed to be known.

3.1. Conflict graph based on protocol model

Let d_{ij} denote the distance between nodes n_i and n_j, R_i be the transmission range of node n_i, and R_i' be the

interference range of node n_i. Note that routing links l_{ij} and l_{pq} are bidirectional links at the MAC and physical layer levels. A routing link l_{ij} is checked eight times against every other routing link while building the conflict graph. An edge is drawn between vertices l_{ij} and l_{pq} if any of the following is true:

- $d_{ip} \leqslant R'_i$ or $d_{iq} \leqslant R'_i$ or $d_{jp} \leqslant R'_j$ or $d_{jq} \leqslant R'_j$ or
- $d_{pi} \leqslant R'_p$ or $d_{pj} \leqslant R'_p$ or $d_{qi} \leqslant R'_q$ or $d_{qj} \leqslant R'_q$.

While constructing the conflict graph based on the protocol model, the interference range is assumed to be twice the transmission range.

3.2. Conflict graph based on SIR model

Unlike the conflict matrix based on the protocol model which consists of ones (indicating conflicts) and zeros (indicating no conflicts), the elements of the conflict matrix for the SIR model are ones and maximum powers received at the link from other links, as shown by the pseudo-code in Fig. 1. The inputs to the conflict graph are as follows:

- *f:* Frequency.
- G_t: Gain of transmitter.
- G_r: Gain of receiver.
- h_t: Transmitter antenna height.
- h_r: Receiver antenna height
- *n:* Number of nodes.
- *RxThresh_dBm:* Receiver threshold in dBm.
- *SIRThresh_dB:* SIR threshold in dB.
- *L:* Set of links involved in routing.
- *locations_x:* Set of *x*-coordinates of nodes.
- *locations_y:* Set of *y*-coordinates of nodes.

Instead of working with four received powers at link l_{xy} from a link l_{pq}, we use the maximum of these received powers to determine the conflict. This significantly reduces the overall computational complexity by reducing the complexity of the related step of the WMaIS stage from $O(m^4)$ to $O(m)$, where m is the number of routing links. *RxThresh_mwatts* is the threshold for power required at the receiver in mW to correctly receive the desired incoming signal. If the ratio of the *RxThresh_mwatts* to the maximum of the four received powers at link l_{xy} from link l_{pq} is less than the SIR threshold, a conflict is indicated between links l_{xy} and l_{pq} by placing a one in the conflict matrix. If this ratio is above the SIR threshold, there can be no conflict between the two links which means that they could both be active simultaneously over the same frequency channel and could potentially become members of the same WMaIS. In this case, the maximum of the four received powers at link l_{xy} from link l_{pq} is placed in the conflict matrix. The worst case computational complexity of our method to construct the conflict graph for this model is $O(n^2 + m + m(m+m)) = O(n^2 + m + 2m^2) \approx O(n^2 + m^2)$, where n is the number of mesh nodes in the network.

The distance between the nodes is calculated using the Euclidean distance formula. The link transmission power or the received interference power is calculated using the Free Space propagation model for short distances and the Two-Ray ground reflection propagation model for longer distances, depending on the Euclidean distance between the nodes $d(x,y)$ in relation to the cross-over distance *Cross_over_dist* [21]. If $d(x,y) \leq$ *Cross_over_dist*, the Free Space propagation model is used, whereas if $d(x,y) >$ *Cross_over_dist*, the Two-Ray propagation model is used. Using the Free Space model, transmission power is calculated as

$$P_t = \frac{RxThresh(4\pi d)^2}{G_t G_r \lambda^2} \tag{1}$$

and received power is calculated as

$$P_r = \frac{P_t G_t G_r \lambda^2}{(4\pi d)^2} \tag{2}$$

Using the Two-Ray model, transmission power is calculated as

$$P_t = \frac{RxThresh(d)^4}{G_t G_r h_t^2 h_r^2} \tag{3}$$

and received power is calculated as

$$P_r = \frac{P_t G_t G_r h_t^2 h_r^2}{(d)^4} \tag{4}$$

where G_t and G_r are transmitter and receiver antenna gain respectively, h_t and h_r are transmitter and receiver antenna height respectively and *RxThresh* is the power threshold required by the radio interface of the receiving node to correctly understand the message [21].

We explain the conflict table and conflict matrix used in Fig. 1 via the following example. Consider the set of links involved in routing L (shown in Table 1) for topology #1 when the node-degree constraint is 3 and the link data rate is 12 Mbps. The corresponding routing graph is shown in Fig. 2. $L(i,1)$ represents the 1st node in the i^{th} link in L, and $L(i,2)$ represents the 2nd node in the i^{th} link in L, for example $L(3,1)$ indicates node 3 and $L(3,2)$ indicates node 1 (i.e. the two nodes in link #3). In Fig. 1, when i is equal to 3 in the *for* loop on line #9, the distance between node 3 and node 1 is stored in $L(3,3)$ and the transmission power for the link $l_{3,1}$ (calculated using (1) or (3)) is stored in $L(3,4)$. $|L| = m = 35$.

In Fig. 1, when *i1* is equal to 3 and j is equal to 14, the entries in the conflict table are as follows and the goal is to find the ratio of *RxThresh_mwatts* and maximum power received at link $l_{3,1}$ (3rd link in L) from link $l_{14,15}$ (14th link in L). Note that the value of *RxThresh_dBm* is -65 dBm and that of *RxThresh_mwatts* is 3.1623×10^{-7} mW. Also for the link data rate of 12 Mbps, the value of *SIRThresh_dB* is 5.78 dB and that of *SIRThresh* is 3.7844.

conflict_table(14,1) = 3 (node 3 in the 3rd link in L, i.e. $l_{3,1}$)
conflict_table(14,2) = 1 (node 1 in the 3rd link in L, i.e. $l_{3,1}$)
conflict_table(14,3) = 14 (node 14 in the 14th link in L, i.e. $l_{14,15}$)
conflict_table(14,4) = 15 (node 15 in the 14th link in L, i.e. $l_{14,15}$)
conflict_table(14,5) = 3.8170×10^{-8} mW (power received at node 3 from node 14)
conflict_table(14,6) = 4.5836×10^{-8} mW (power received at node 3 from node 15)

Inputs:
- f, G_t, G_r, h_t, h_r, n, *RxThresh_dBm*, *SIRThresh_dB*, L, *locations_x*, *locations_y*.

Output:
- *conflict_matrix*: Conflict graph

BEGIN
1. $RxThresh\_mwatts \leftarrow 10^{(RxThresh\_dBm/10)}$
2. $SIRThresh \leftarrow 10^{(SIRThresh\_dB/10)}$
3. $m \leftarrow |L|$
4. ***For*** i=1 to n:
5. ***For*** j=1 to n:
6. $dist\_all(i,j) \leftarrow$ the distance between node i and node j
7. ***end For***
8. ***end For***
9. ***For*** i=1 to m:
10. $L(i,3) \leftarrow$ the distance between the nodes of link i
11. $L(i,4) \leftarrow$ the transmission power for link i using (1) or (3)
12. ***end For***
13. Initialize an $m \times m$ *conflict_matrix* of all ones
14. ***For*** $i1$=1 to m:
15. Initialize an empty conflict table
16. ***For*** j=1 to m:
17. $conflict\_table(j,1) \leftarrow$ node x of link $i1$
18. $conflict\_table(j,2) \leftarrow$ node y of link $i1$
19. $conflict\_table(j,3) \leftarrow$ node p of link j
20. $conflict\_table(j,4) \leftarrow$ node q of link j
21. $P_{r,xp} \leftarrow$ the power received at node x of link $i1$ from node p of link j using (2) or (4)
22. $P_{r,xq} \leftarrow$ the power received at node x of link $i1$ from node q of link j using (2) or (4)
23. $P_{r,yp} \leftarrow$ the power received at node y of link $i1$ from node p of link j using (2) or (4)
24. $P_{r,yq} \leftarrow$ the power received at node y of link $i1$ from node q of link j using (2) or (4)
25. $conflict\_table(j,5) \leftarrow P_{r,xp}$
26. $conflict\_table(j,6) \leftarrow P_{r,xq}$
27. $conflict\_table(j,7) \leftarrow P_{r,yp}$
28. $conflict\_table(j,8) \leftarrow P_{r,yq}$
29. $conflict\_table(j,9) \leftarrow \max(P_{r,xp}, P_{r,xq}, P_{r,yp}, P_{r,yq})$
30. $conflict\_table(j,10) \leftarrow RxThresh\_mwatts / \max(P_{r,xp}, P_{r,xq}, P_{r,yp}, P_{r,yq})$
31. ***end For***
32. ***For*** $i2$=1 to m:
33. ***If*** $conflict\_table(i2,10) > SIRThresh$:
34. $conflict\_matrix(i1,i2) \leftarrow conflict\_table(i2,9)$
35. ***end If***
36. ***end For***
37. ***end For***
38. Output *conflict_matrix*

END

Fig. 1. Conflict graph based on SIR model.

Table 1
Set of links involved in routing for topology #1.

No.	Link		No.	Link		No.	Link		No.	Link		No.	Link		No.	Link		No.	Link	
1	1	8	**6**	6	5	**11**	11	17	**16**	17	16	**21**	22	16	**26**	27	21	**31**	32	26
2	2	1	**7**	7	14	**12**	12	24	**17**	18	24	**22**	23	22	**27**	28	22	**32**	33	27
3	3	1	**8**	8	13	**13**	13	14	**18**	19	13	**23**	24	23	**28**	29	28	**33**	34	27
4	4	3	**9**	9	2	**14**	14	15	**19**	20	19	**24**	25	19	**29**	30	35	**34**	35	34
5	5	11	**10**	10	17	**15**	16	15	**20**	21	15	**25**	26	21	**30**	31	32	**35**	36	35

$conflict\_table(14,7) = 4.7488 \times 10^{-8}$ mW (power received at node 1 from node 14)
$conflict\_table(14,8) = 3.7730 \times 10^{-8}$ mW (power received at node 1 from node 15)
$conflict\_table(14,9) = 4.7488 \times 10^{-8}$ mW (maximum power received at $l_{3,1}$ from $l_{14,15}$)
$conflict\_table(14,10) = 6.6591$ (ratio of *RxThresh_mwatts* and maximum power received at $l_{3,1}$ from $l_{14,15}$)

Note that the transmission power for $l_{14,15}$ (calculated earlier and stored in $L(14,4)$) is used while calculating the received powers at $l_{3,1}$ from $l_{14,15}$ in the conflict table. The relevant entry in the conflict matrix when $i2$ is equal to 14 is

$$conflict\_matrix(3,14) = 4.7488 \times 10^{-8} \text{ mW},$$

since the ratio of the *RxThresh_mwatts* and maximum power received at $l_{3,1}$ from $l_{14,15}$ is 6.6591, which is greater than the required SIR threshold of 3.7844. This maximum received power at $l_{3,1}$ from $l_{14,15}$ is used later while building weighted maximal independent sets during the minimum coloring stage.

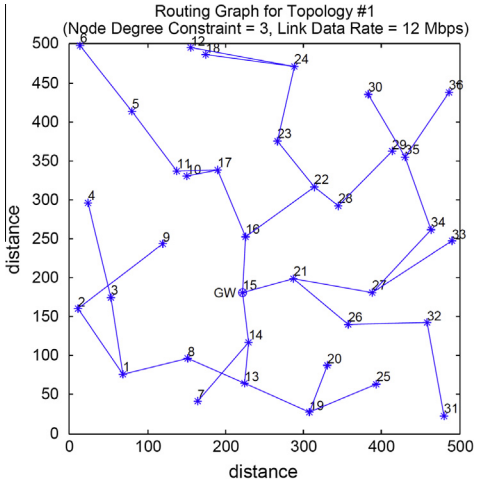

Fig. 2. Routing graph for topology #1.

Similarly, when we check the maximum power received at $l_{17,16}$ (16^{th} link in L) from $l_{23,22}$ (22^{nd} link in L), we find it to be 2.5086×10^{-7} mW which results in

$$conflict\_matrix(16,22) = 1,$$

since the ratio of the *RxThresh_mwatts* and maximum power received at $l_{17,16}$ from $l_{23,22}$ is 1.2606 which is less than the required SIR threshold of 3.7844. This value of 1 indicates a conflict between links $l_{17,16}$ and $l_{23,22}$ which means that these two links cannot be active simultaneously over the same frequency channel. Note that for two links l_{xy} (link number s in L) and l_{pq} (link number t in L), a one in either or both $conflict\_matrix(s,t)$ and $conflict\_matrix(t,s)$ indicates a conflict between these links.

3.3. Conflict graph based on SIR model with shadowing

The conflict graph for the SIR model is extended to include shadowing. The transmission power using the Free Space model with shadowing is calculated as

$$P_t = \frac{RxThresh(4\pi d)^2}{G_t G_r \lambda^2} \times 10^{-x/10} \tag{5}$$

where x is the lognormal random variable. The transmission power using the Two-Ray model with shadowing is calculated as

$$P_t = \frac{RxThresh(d)^4}{G_t G_r h_t^2 h_r^2} \times 10^{-x/10} \tag{6}$$

While creating the conflict matrix for the SIR model with shadowing, the link transmission power is calculated using either (5) or (6), depending on the cross-over distance. The inputs for the conflict graph for this model, in addition to those in the pseudo-code in Fig. 1, include the standard deviation for shadowing σ and the outage probability *OP*.

If p_c is the probability that the received power P_r is greater than or equal to the receiver threshold *RxThresh*, then the outage probability *OP* is $(1 - p_c)$. Consider the following example where we find the transmission power P_t for a 100 m long link between two nodes using (5) such that the probability that $P_r \geqslant RxThresh$ is 90%. In other words, the outage probability *OP* is 10%. In this example, we have $f = 5.805$ GHz, $G_t = 1$, $G_r = 1$, $RxThresh = -65$ dBm and $\sigma = 3$ dB. Using (5), we proceed as follows.

$$RxThresh + 20\log(4\pi d) = 10\log P_t + 10\log G_t + 10\log G_r + 20\log\lambda + \frac{x}{10}(10\log 10)$$

$$-65 + 61.9842 = 10\log P_t + 0 + 0 - 25.7336 + x$$

$$x = 22.7178 - 10\log P_t$$

Now $\mathbb{P}(P_r \geqslant RxThresh) \geqslant 0.9$ can be written in terms of Q-function as

$$Q\left(\frac{z-u}{\sigma}\right) \geqslant 0.9$$

$$Q\left(\frac{22.7178 - 10\log P_t}{3}\right) \geqslant 0.9$$

Since $1 - Q(-z) = Q(z)$, the above equation can be written as

$$1 - Q\left(\frac{10\log P_t - 22.7178}{3}\right) \geqslant 0.9$$

$$Q\left(\frac{10\log P_t - 22.7178}{3}\right) \leqslant 0.1$$

For $Q(z) \leqslant 0.1$, we find that $z \geqslant 1.2816$ from the Q-function table. The above equation can now be written as

$$\frac{10\log P_t - 22.7178}{3} \geqslant 1.2816$$

$$10\log P_t \geqslant 26.5626$$

$$P_t \geqslant 453.1688$$

Hence, using the Free Space model with shadowing, a transmission power of 453.1688 mW is required for a 100 m link to achieve an *OP* of 10% at the receiver when the operating frequency is 5.805 GHz and the standard deviation for shadowing is 3 dB. Decreasing the outage probability will result in an increase in the transmission power required. For example, decreasing the outage probability to 5% in the above example will increase the transmission power to 582.422 mW. Also, an increase in σ will lead to an increase in the transmission power required. For example, increasing σ to 5 dB in the above example will increase the transmission power to 817.6312 mW.

4. Channel assignment problem

4.1. Network architecture

In a WMN, an access point that is connected to the wired network is called a *gateway*; access points without wired connections are called *mesh routers* (MRs) and connect to the GW through multiple hops. MRs and GWs are similar in design, with the only difference that a GW is

directly connected to the wired network while a MR is not. Mesh nodes have no power constraint and have abundant power at their disposal [22]. In this work, we assume a single GW that is always available and that cannot fail like a mesh router. We plan to extend our work to multiple GWs where in the case of a GW failure, the remaining GW or GWs can serve as a fallback toward failure recovery.

Each mesh node is assumed to be equipped with multiple radio interfaces. One of these radios is used for control traffic, while the others are used for data traffic. We define the *node-degree* of a mesh node as the number of neighbors it can communicate with simultaneously for data communication. For example, a node-degree constraint of two means that each mesh node is equipped with two radio interfaces for data traffic, and can communicate with at most two of its neighbors at the same time. The radio interfaces are assumed to be half duplex and each is equipped with an omni-directional antenna. We assume that the radio interfaces at nodes can be tuned to different non-overlapping frequency channels. For communication of the control traffic, the control radios of all nodes are tuned to a common frequency channel.

4.2. Connectivity graph

In the connectivity graph $C(V,E)$, vertices V correspond to wireless nodes and the edges E correspond to the wireless links between the nodes. We use our *Select x for less than x* TCA to build the connectivity graph. Our TCA mitigates co-channel interference and enhances spatial channel reuse while ensuring network connectivity. It controls the network topology by selecting the nearest neighbors for each node. Since transmit power is proportional to the distance between the nodes, the shorter the distance, the lower the transmit power. Less transmit power translates to less interference which leads to better spatial channel reuse.

Each mesh router broadcasts a *Hello* message at maximum power containing its node ID and position over the control frequency channel using the control radio. From the information in the received *Hello* messages, each MR arranges its neighboring nodes in ascending order of their distance. The result is the *maximum power neighbor table* (MPNT). Then each MR sends its MPNT along with its position and node ID to the GW over the control channel. For each MR in the network, the gateway builds a *direct neighbor table* by selecting at least x nearest nodes for that mesh router, and then converts the uni-directional links in the direct neighbor table of a mesh node into bi-directional links, which results in the *final neighbor table*. Bi-directional links are required for link level acknowledgments and to ensure the existence of reverse paths. The connectivity graph is constructed using the final neighbor table. Node locations are assumed to be known. To achieve a strongly connected topology, we assume a maximum transmission range of 164 m for all mesh nodes.

4.3. Multi-path routing

We formulate the multi-path routing problem in multi-radio WMNs as a mixed integer linear program. We call the index $p \in P$ a commodity. Let:

- P be the commodities, i.e. source-sink pairs $(s_1, t_1), \ldots, (s_P, t_P)$,
- f_{ij}^p be a variable denoting the amount of flow of commodity p on link l_{ij},
- f_s^p be a variable denoting the amount of inflow of commodity p from the source of p,
- f_d^p be a variable denoting the amount of outflow of commodity p from the sink of p,
- c_{ij} be an input parameter denoting the capacity of link l_{ij} where $l_{ij} \in E$, such that $c_{ij} \in \{9.18, 15.52, 20.03, 24.73\}$,
- z_{ij} be a binary variable such that $z_{ij} \in \{0, 1\}$ is 1 when the link l_{ij} is used for routing and 0 otherwise,
- dc be an input parameter denoting the constraint on the node-degree of the mesh routers, such that $dc \in \{2, 3, 4, 5, 6\}$,
- $cost_{ij}$ be an input parameter containing a cost of 0.0001 for each link l_{ij},
- $demand_{sd}$ be an input parameter representing flow demands between the source-sink pairs and is equal to 1 for all commodities, and
- y be a variable denoting the multiplier on the unit flow demand of the commodities.

We assume a value for the link capacity based on the fact that maximum goodputs (maximum link throughputs) of an IEEE 802.11a link operating at data rates of 12, 24, 36 and 54 Mbps are 9.18, 15.52, 20.03, and 24.73 Mbps, respectively [23].

4.3.1. Objective

$$max\left(y - \sum_{l_{ij} \in E}(z_{ij} \times \text{cost}_{ij})\right) \tag{7}$$

Given the connectivity graph, the link capacity, the node-degree constraint and the unit flow demand between the source-sink pairs, the objective is to maximize y, which is the multiplier on the unit flow demand of the commodities, so as to achieve the maximum total flow in the network using multiple paths between a source-sink pair. In this work, the *maximum network throughput* means the maximum possible total network flow, i.e. the maximum possible flow that can reach the GW from all sources. Since the flow demand between all source-sink pairs is 1 and y is the multiplier on this flow demand, y also represents the amount of flow from each source reaching the GW. We need y in the multi-path routing formulation to implement fairness. By maximizing y, we ensure that the flow from each source reaching the GW is maximized equally.

The small value of $cost_{ij}$ in (7) prevents redundant flow-loops and does not affect the result.

4.3.2. Constraints

The following are the flow balance constraints for the source nodes, sink (GW) node and the intermediate nodes, respectively. For the source nodes (or the sink node), the sum of the outgoing flow of a commodity is equal to the sum of incoming flow for that commodity and the amount of inflow (or outflow) of that commodity from the source (or sink) of that commodity. For the intermediate nodes,

the sum of the incoming flow of a commodity is equal to the sum of the outgoing flow for that commodity:

$$\sum_j f_{sj}^p - \sum_i f_{is}^p - f_s^p = 0, \quad \text{for all } p \text{ and for all } s \tag{8}$$

where $s, i, j \in V$,

$$f_d^p + \sum_i f_{id}^p - \sum_j f_{dj}^p = 0, \quad \text{for all } p \text{ and for all } d \tag{9}$$

where $d, i, j \in V$,

$$\sum_j f_{ji}^p - \sum_k f_{ik}^p = 0, \quad \text{for all } p \text{ and for all } i \tag{10}$$

where $i \in V \setminus \{s_p, d_p\}$, $j, k \in V$, and $p \in P$.

The following represent the constraints on the node-degree of the mesh routers in the WMN. At any mesh node in the network, there is a limit on the number of radio-interfaces and hence on the number of incoming plus outgoing links. If the limit is 4, i.e. if $dc = 4$, then at each mesh node n_i,

$$\sum_k z_{ki} + \sum_j z_{ij} \leqslant 4, \quad \text{for all } i \tag{11}$$

where $i, j, k \in V$.

The maximum total flow in the network depends on the number of links for the GW (sink) node for a certain node-degree constraint. Varying x in the *Select x for less than x* TCA for different node-degree constraints ensures that the total amount of flow in the network increases with an increase in the node-degree constraint. It creates a certain amount of connectivity for a given node-degree constraint and hence, a certain number of links for the GW. For node-degree constraints of 2 and 3 we use the *Select 3 for less than 3* TCA to ensure at least 3 links for the GW in the connectivity graph; for a node-degree constraint of 4 we use the *Select 4 for less than 4* TCA to ensure at least 4 links for the GW in the connectivity graph, and so on. Since *Select 2 for less than 2* TCA mostly leads to a disconnected network in the case of random and controlled random topologies, we use *Select 3 for less than 3* TCA in this case.

The following constraints introduce fairness among flows of the multiple commodities. A change in y (the multiplier on the unit flow demand of the commodities) ensures that the inflows for all commodities are changed equally:

$$f_s^p \geqslant y \times demand_{sd}, \quad \text{for all } p \text{ and for all } s \text{ and } d \tag{12}$$

where $s \in \{sources\}$, $d \in \{sinks\}$, and $p \in P$.

The following constraints represent the half-duplex nature of the radio-interfaces of the mesh routers in which a link can be used for either transmission or reception but not for both:

$$z_{ij} + z_{ji} \leqslant 1, \quad \text{for all } i \text{ and } j \tag{13}$$

where $i, j \in V$.

The following are the link capacity constraints that ensure that the sum of flows of commodities on a link does not exceed the link capacity:

$$\sum_p f_{ij}^p \leqslant c_{ij} \times z_{ij}, \quad \text{for all } p \text{ and for all } i \text{ and } j \tag{14}$$

where $i, j \in V$, and $p \in P$.

The link capacities cannot be negative:

$$c_{ij} \geqslant 0, \quad \text{for all } i \text{ and } j \tag{15}$$

where $i, j \in V$.

The flow of a commodity p on a link is non-negative but is not required to be an integer:

$$f_{ij}^p \geqslant 0, \quad \text{for all } p \text{ and for } i \text{ and } j \tag{16}$$

where $i, j \in V$, and $p \in P$.

We use the AMPL language [24] to model the multi-path routing problem, and IBM CPLEX 12.2 [25] to solve the resulting problem. We set *mipemphasis* = 1 in CPLEX and ask it to search for the first feasible solution. This significantly reduces the solution time at the cost of a small degradation in the network throughput. If the solver cannot find a solution of the multi-path routing problem for node-degree constraints of 2 or 3, we move to a higher TCA to build the connectivity graph, i.e. *Select 4 for less than 4* TCA or *Select 5 for less than 5* TCA, until the first feasible solution is found.

4.4. Minimum coloring problem

A coloring of the conflict graph F is an assignment of colors (frequency channels) to vertices such that adjacent vertices receive different colors. The *minimum coloring problem* is to find a coloring of the vertices in the conflict graph F using as few distinct colors as possible; this is the same as the problem of finding the minimum number of frequency channels to use such that there is no interference.

The minimum coloring problem is NP-hard for general graphs [3]. Our proposed greedy heuristic for the solution of this problem consists of these steps: (1) find a maximal independent set (MaIS) (or a WMaIS) of vertices and assign the members of this set to the same frequency channel, (2) remove these vertices from the conflict graph, and (3) repeat until all vertices are colored (assigned a frequency channel). The number of frequency channels needed for interference-free communication among the mesh nodes is equal to the number of MaISs (or WMaISs). Since finding a maximum independent set is itself NP-hard [26], we use heuristics for the solution of this step of the channel assignment problem.

4.4.1. Heuristic algorithms using MaISs

For the conflict graph generated based on the protocol model, we use the following three heuristic algorithms, based on the classic greedy approach. Algorithm 1 starts by selecting a vertex from the conflict graph with the maximum node-degree and introduces that vertex into the maximal independent set under construction. The algorithm then checks the other vertices of the conflict graph one by one and puts them in the set if they do not have an edge connecting to any of the vertices already in the set. To construct the next MaIS, the algorithm deletes the members of the previous MaIS from the conflict graph. Algorithm 2 starts by selecting a vertex from the conflict graph with the minimum node-degree. Algorithm 3 starts by selecting a vertex at random from the conflict graph.

4.4.2. Heuristic algorithms using WMaISs

For the conflict graph generated based on the SIR model or the SIR model with shadowing, we enhance the above heuristic algorithms to find weighted maximal independent sets. These must respect the constraint that the cumulative SIR at every vertex in a WMaIS must be greater than the SIR threshold, where the *cumulative SIR* at a vertex is the ratio of *RxThresh_mwatts* to the sum of the maximum powers received at that vertex from all other vertices in the WMaIS. This accounts for the cumulative interference at a vertex in the WMaIS from all other vertices in this set. The pseudo-code for *Enhanced Algorithm 1* is shown in Fig. 3. If a vertex w does not conflict with vertices already in the WMaIS under construction, we add w and the vertices in the WMaIS to a temporary set. If the cumulative SIR at every vertex in the temporary set from all other vertices in this set is greater than the SIR threshold, we add w to the WMaIS. The worst case computational complexity of our algorithm is $O(m(m+m)) = O(m \times 2m) \approx O(m^2)$.

We explain how to build a WMaIS with the help of an example. The goal is to assign frequency channels to links in L (the set of links involved in routing) such that all of these links can be active simultaneously, which means finding WMaISs in the conflict graph for these links. Consider the L shown in Table 1. From the conflict graph based on the conflict matrix for L, we select the vertex with the maximum node degree, i.e. the vertex in the conflict graph having the most conflicts with other vertices in the conflict graph, and add it to an empty WMaIS. This is vertex number 20 in the conflict graph, i.e. the twentieth link in L which is $l_{21,15}$; so the current WMaIS is $V_{WMaIS} = \{20\}$. Vertex 20 conflicts with 28 other vertices (including itself) and has no conflict with the following 7 vertices in the conflict graph: vertex 6 (link $l_{6,5}$ in L), vertex 10 (link $l_{10,17}$ in L), vertex 11 (link $l_{11,17}$ in L), vertex 12 (link $l_{12,24}$ in L), vertex 17 (link $l_{18,24}$ in L), vertex 29 (link $l_{30,35}$ in L), vertex 35 (link $l_{36,35}$ in L).

In the next step, we put vertex 20 ($l_{21,15}$) and vertex 6 ($l_{6,5}$) in a temporary set. Since the ratio of *RxThresh_mwatts*

Inputs:
- L: set of links involved in routing
- $F(V_F, E_F)$: conflict graph
- *SIRThresh_dB*: SIR threshold in dB
- *RxThresh_dBm*: Receiver threshold in dBm

Outputs:
- V_{WMaIS}: WMaIS of vertices
- L_{WMaIS}: Set of links in L corresponding to vertices in WMaIS
- c: number of WMaISs

BEGIN
1. $c \leftarrow 0$
2. $m \leftarrow |L| = |V_F|$
3. $SIRThresh \leftarrow 10^{(SIRThresh\_dB/10)}$
4. $RxThresh\_mwatts \leftarrow 10^{(RxThresh\_dBm/10)}$
5. ***While*** $m \geq 1$:
6. ***If*** F is fully connected or m=1:
7. ***For*** d=1 to m:
8. Initialize an empty V_{WMaIS} and L_{WMaIS}
9. Add *vertex* d to V_{WMaIS} and the corresponding link to L_{WMaIS}
10. Output V_{WMaIS} and L_{WMaIS}
11. $c \leftarrow c+1$
12. ***end For***
13. Output c and exit
14. ***end If***
15. Initialize an empty V_{WMaIS} and L_{WMaIS}
16. Add *vertex* of F with the maximum node-degree to V_{WMaIS} and the corresponding link to L_{WMaIS}
17. ***For*** i=1 to m:
18. ***If*** vertex i does not have an edge with vertices in V_{WMaIS}:
19. $V_{temp} \leftarrow V_{WMaIS} \cup i$
20. ***end If***
21. ***If*** the cumulative SIR at every vertex in V_{temp} from all other vertices in V_{temp} is greater than *SIRThresh*:
22. Add *vertex* i to V_{WMaIS} and the corresponding link to L_{WMaIS}
23. ***end If***
24. ***end For***
25. Output V_{WMaIS} and L_{WMaIS}
26. $c \leftarrow c+1$
27. $V_F \leftarrow V_F \setminus V_{WMaIS}$
28. $L \leftarrow L \setminus L_{WMaIS}$
29. $m \leftarrow |L|$
30. ***end While***
31. Output c

END

Fig. 3. Enhanced Algorithm 1 for WMaISs.

(3.1623×10^{-7} mW) and the maximum power received at $l_{21,15}$ from $l_{6,5}$ (4.8471×10^{-8} mW) is 6.5241 which is above the required SIR threshold of 3.7844, and since the ratio of *RxThresh_mwatts* and the maximum power received at $l_{6,5}$ from $l_{21,15}$ (1.9321×10^{-8} mW) is 16.3671 which is also above the required SIR threshold, we add vertex 6 to the WMaIS. Now the current WMaIS is $V_{WMaIS} = \{6, 20\}$. Note that the maximum received powers are available to us from the conflict matrix.

Vertices 10, 11, 12 and 17 cannot become members of the current WMaIS because they conflict with vertex 6 in the conflict graph, which is a member of the current WMaIS.

Next we put vertex 6 ($l_{6,5}$), vertex 20 ($l_{21,15}$), and vertex 29 ($l_{30,35}$) in a temporary set and check the cumulative SIR at every vertex. First, we check for cumulative SIR at $l_{6,5}$. The maximum power received at $l_{6,5}$ from $l_{21,15}$ is 1.9321×10^{-8} mW and from $l_{30,35}$ is 3.0049×10^{-8} mW, totaling 4.937×10^{-8} mW. The ratio of *RxThresh_mwatts* and the cumulative maximum received power is 6.4053 which is above the required SIR threshold of 3.7844. Second, we check for cumulative SIR at $l_{21,15}$. The maximum power received at $l_{21,15}$ from $l_{6,5}$ is 4.8471×10^{-8} mW and from $l_{30,35}$ is 6.1925×10^{-8} mW, totaling 11.0396×10^{-8} mW. The ratio of *RxThresh_mwatts* and the cumulative maximum received power is 2.8645. This ratio is below the required SIR threshold, so vertex 29 ($l_{30,35}$) cannot become a member of the current WMaIS. Note that we would have checked for the cumulative SIR at vertex 29 ($l_{30,35}$) if the cumulative SIR at vertex 20 ($l_{21,15}$) had been above the required SIR threshold.

Lastly we put vertex 6 ($l_{6,5}$), vertex 20 ($l_{21,15}$), and vertex 35 ($l_{36,35}$) in a temporary set and check the cumulative SIR at every vertex. First, we check for cumulative SIR at $l_{6,5}$. The maximum power received at $l_{6,5}$ from $l_{21,15}$ is 1.9321×10^{-8} mW and from $l_{36,35}$ is 2.5448×10^{-8} mW, totaling 4.4769×10^{-8} mW. The ratio of *RxThresh_mwatts* and the cumulative maximum received power is 7.0636 which is above the required SIR threshold of 3.7844. Second, we check for cumulative SIR at $l_{21,15}$. The maximum power received at $l_{21,15}$ from $l_{6,5}$ is 4.8471×10^{-8} mW and from $l_{36,35}$ is 7.1585×10^{-8} mW, totaling 12.0056×10^{-8} mW. The ratio of *RxThresh_mwatts* and the cumulative maximum received power is 2.6340. Since this ratio is below the required SIR threshold, vertex 35 ($l_{36,35}$) cannot become a member of the current WMaIS. In this way, we construct the first WMaIS as $V_{WMaIS} = \{6, 20\}$. This means that the links $l_{6,5}$ and $l_{21,15}$ in L can be active simultaneously and are assigned the same frequency channel.

These heuristics to find MaISs (or WMaISs) are very quick, so we run each of them 25 times on the conflict graph and take the best solution over all 75 runs.

The procedures related to the connectivity graph, routing, conflict graph and minimum coloring heuristic are carried out at the GW, which then sends each MR its channel assignment and routing information over the control channel using the control radio. Based on the channel assigned to a MR for communication with a neighbor and its distance to that neighbor, each MR applies power control and adjusts its transmission power accordingly by using the appropriate propagation model.

Our channel assignment method supports a dynamic WMN environment that undergoes regular topological changes as new mesh nodes join the network or existing mesh nodes leave it (e.g. due to node failure). To achieve this, all mesh nodes exchange periodic *keep-alive* messages using maximum transmission power on the control frequency channel using their control radios. The *keep-alive* message from a node which contains its node ID and its position tells its neighbors within its maximum transmission range that the node is active. If a mesh node fails then its maximum-transmission-range neighbors will not receive its periodic *keep-alive* message. After receiving *keep-alive* messages from its neighbors, a mesh node builds a new MPNT using the information received from these messages and sends its MPNT along with its position and node ID to the GW over the control frequency channel. Based on the received MPNTs, the GW performs a new channel assignment and sends this information to all mesh nodes in the network on the control frequency channel. Each mesh router receives the new channel assignment information on the control frequency channel over its control radio and switches its radios to new frequency channels in case the received channel assignment is different from its existing channel assignment. If a new mesh node joins the network, it sends a *Hello* message using maximum transmission power to inform mesh nodes within its maximum transmission range of its presence. Note that a *Hello* message is the same as a *keep-alive* message but has a different name as it is used to announce the presence of a new node. Whenever there is a topology change as an existing mesh router leaves/fails or a new mesh router joins the network, the exchange of *keep-alive* or *Hello* messages over the common control frequency channel in combination with the low computational complexity of our channel assignment method will lead to a quick reassignment of frequency channels and a fast reconfiguration of the network.

If a data radio is used for control traffic, it will have to switch to the control frequency channel every time it has to send control information. The delay caused by channel switching and transmission of control information will disrupt the data traffic on the link [27]. For this reason, we propose the use of a dedicated control radio on every mesh node for control traffic. The cost of multiple radios is no longer a prohibitive factor due to the decreasing cost of wireless interface cards [28].

Because of the ad hoc nature of the mesh network, communication between mesh nodes is not synchronized, so a dedicated time slot cannot be used as the control channel. Instead we dedicate a frequency channel as the common control channel for the exchange of control traffic. This allows us to achieve interference-free communication among the mesh nodes, but at the cost of occupying a frequency channel. A data frequency channel should not be used for control traffic as this will cause severe interference for those links using the same frequency channel for data traffic because the *keep-alive* as well as *Hello* messages are sent using maximum transmission power.

One can argue that the control radio can be used for some data transmissions to increase the overall throughput of the system. The idle time on the control interface

can be used to transmit some data traffic. In a simple scheme, some data traffic can also be carried on the control interface in addition to the control traffic by using random access over the control frequency channel.

5. Performance evaluation

We evaluate the performance of the three interference models for network throughput (NT) at different node-degree constraints (NDCs) based on the number of frequency channels required (NCR). For constructing the conflict graph based on the SIR model and the SIR model with shadowing, we assume the frequency to be 5.805 GHz, G_t and G_r to be 1, h_t and h_r to be 3 m, and receiver threshold to be −65 dBm. As mentioned earlier, we assume a capacity for each link based on its maximum goodput at a particular link data rate. The SIR requirements for different data rates are shown in Table 2. As per the IEEE 802.11a standard [29], a symbol duration of 4 μs and an occupied bandwidth of 16.6 MHz is used while calculating the required SIR. We use these reasonable assumptions to generate representative results, but our work can be applied to any scenario of multi-hop MRMC WMNs and is not limited to any specific standard.

5.1. Network topology

A controlled random topology (CRT) has been used for the evaluation, in which a 500 m × 500 m physical terrain is divided into cells and a MR is placed randomly within each cell according to a uniform random distribution. Twenty-five different CRTs consisting of 36-node networks are considered. Irrespective of its location, Node 15 is set to be the GW for all CRTs. As stated earlier, all mesh nodes except the GW are set as sources of flow (i.e. data traffic). The flow from each source can take multiple paths to the GW, which is the sink for all flows. In other words, there are 35 source-sink pairs and 35 flows in the network.

5.2. Numerical results for network throughout

The amount of flow for each commodity reaching the GW (sink) is equal to y times $demand_{sd}$ as per (12). However, due to a unit flow demand between each source-sink pair, the value of y in Table 3 represents the amount of flow from each source reaching the GW. This indicates that all of the 35 flows in the network are maximized equally. For a NDC of 2 in Table 3 at a link capacity of 24.73 Mbps for a data rate of 54 Mbps, y is 1.1270. The network throughput, i.e. the total amount of flow in the network, is equal to the number of sources times y, i.e. 35 × 1.1270 = 39.45 Mbps.

The link capacity (maximum link throughput) for a particular IEEE 802.11a link data rate is calculated using [23]

$$MT = \frac{8 \times L_{DATA}}{T_{D\_DATA} + T_{D\_ACK} + 2\tau + T_{DIFS} + T_{SIFS} + \overline{CW}} \quad (17)$$

Table 2
SIR requirement for different data rates.

Link data rate (Mbps)	Modulation	Code rate	Coded bits per symbol	Coded Eb/No (dB) [30]	Required SIR (dB)
12	QPSK	1/2	96	4.18	**5.78**
24	16-QAM	1/2	192	6.32	**10.93**
36	16-QAM	3/4	192	8.59	**13.20**
54	64-QAM	3/4	288	12.04	**18.41**

Table 3
Network throughput.

Link data rate (Mbps)	NDC	y	NT (Mbps)	95% CI for NT (Mbps)	Maximum NT (Mbps)
12	2	0.4497	**15.74**	15.00–16.48	**18.36**
	3	0.7079	**24.78**	22.93–26.63	**27.54**
	4	0.9029	**31.60**	29.80–33.40	**36.72**
	5	1.2466	**43.63**	41.86–45.40	**45.90**
	6	1.5063	**52.72**	49.99–55.45	**55.08**
24	2	0.7259	**25.40**	23.77–27.04	**31.04**
	3	1.2406	**43.42**	40.55–46.29	**46.56**
	4	1.5634	**54.72**	50.96–58.47	**62.08**
	5	2.1075	**73.76**	70.86–76.67	**77.60**
	6	2.5350	**88.72**	85.37–92.08	**93.12**
36	2	0.9265	**32.43**	30.47–34.39	**40.06**
	3	1.6281	**56.98**	54.76–59.20	**60.09**
	4	1.9580	**68.53**	63.93–73.13	**80.12**
	5	2.7212	**95.24**	91.16–99.32	**100.15**
	6	3.2263	**112.92**	107.89–117.95	**120.18**
54	2	1.1270	**39.45**	37.10–41.80	**49.46**
	3	2.0302	**71.06**	68.63–73.48	**74.19**
	4	2.5764	**90.17**	84.76–95.59	**98.92**
	5	3.3913	**118.70**	113.61–123.79	**123.65**
	6	3.8762	**135.67**	127.25–144.08	**148.38**

$$T_{D\_DATA} = T_P + T_{PHY} + T_{SYM} \times \left\lceil \frac{16 + 6 + (8 \times L_{H\_DATA}) + (8 \times L_{DATA})}{N_{DBPS}} \right\rceil \quad (18)$$

$$T_{D\_ACK} = T_P + T_{PHY} + T_{SYM} \times \left\lceil \frac{16 + 6 + (8 \times L_{ACK})}{N_{DBPS}} \right\rceil \quad (19)$$

$$\overline{CW} = \frac{CW_{\min} \times T_{slot}}{2} \quad (20)$$

where

MT is the maximum link throughput in bps;
L_{DATA} is the length of the payload in bytes;
T_{D_DATA} is the data transmission delay;
T_{D_ACK} is the ACK (acknowledgment) transmission delay;
τ is the propagation delay and is equal to 1 μs for 802.11a;
T_{SIFS} is the SIFS time and is equal to 16 μs for 802.11a;
T_{DIFS} is the DIFS time and is equal to 34 μs for 802.11a;
$\overline{CW}$ is the average backoff time;
T_P is transmission time of physical preamble and is equal to 16 μs for 802.11a;
T_{PHY} is the transmission time of the PHY header and is equal to 4 μs for 802.11a;
T_{SYM} is the transmission time for a symbol and is equal to 4 μs for 802.11a;
L_{H_DATA} is the MAC overhead in bytes and is equal to 28 bytes;
L_{ACK} is the ACK size in bytes and is equal to 28 bytes;
N_{DBPS} is the number of data bits per symbol;
CW_{min} is the minimum backoff window size and is equal to 15 for 802.11a; and
T_{slot} is the slot time and is equal to 9 μs for 802.11a.

Substituting (18)–(20) in (17) and simplifying, we get

$$MT = \frac{8 \times L_{DATA}}{159.5 + 4 \times \left\lceil \frac{246}{N_{DBPS}} \right\rceil + 4 \times \left\lceil \frac{246 + (8 \times L_{DATA})}{N_{DBPS}} \right\rceil} \times 10^6 \quad (21)$$

Using (21) and assuming a payload size of 1000 bytes, the maximum link throughput for the link data rate of 54 Mbps (N_{DBPS} = 216) is found to be 24.73 Mbps.

The total amount of flow in the network depends on the number of links for the GW node, which increases with an increase in the NDC. For example, at a link capacity of 24.73 Mbps for a data rate of 54 Mbps, the maximum network throughput is 49.46 Mbps for a NDC of 2, or 74.19 Mbps for a NDC of 3, and so on. The results in Table 3 indicate that the network throughput increases with an increase in the NDC. However, there is a small degradation in the achieved network throughput as compared to its maximum value due to finding the first feasible solution vs. finding the optimum solution.

5.3. Numerical results for NCR

We collected mean values and statistics on the 95% confidence intervals (CIs) of the NCR for the 25 different CRTs used. Since the confidence intervals for different NDCs are tightly grouped around the mean, they are not reported in a table. The mean values are graphed so that trends are immediately apparent.

In Figs. 4–8, γ represents the required SIR threshold, σ represents the standard deviation for shadowing and OP represents the outage probability. Note that the red line in Figs. 4, 7 and 8 represents the maximum value of NCR. This is the worst case scenario in which each link involved in routing requires a different frequency channel. For example, if the number of links involved in routing for a CRT is 35, then the number of frequency channels required is also 35 in the worst case scenario.

5.3.1. Comparison of the three interference models

Fig. 4 provides a comparison of the three interference models based on NCR for a link data rate of 24 Mbps. γ is 10.93 dB, σ is 3 dB and OP is 10%. The simplistic protocol model has the lowest NCR among the three models. The SIR model with shadowing is the most realistic of the

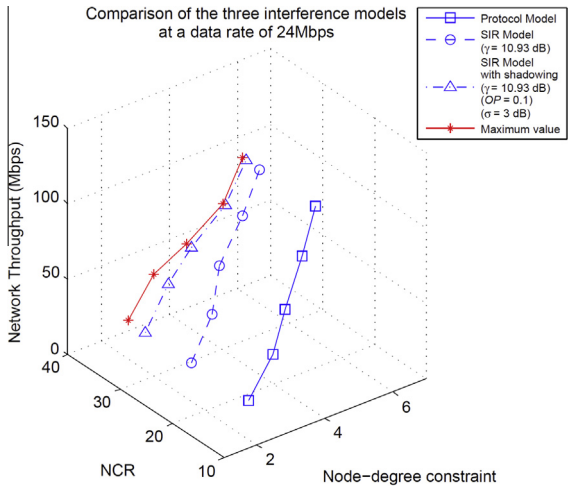

Fig. 4. NCR – comparison of the three interference models at a link data rate of 24 Mbps.

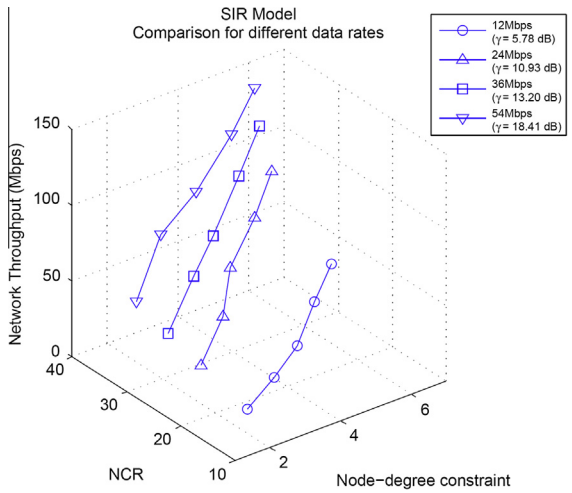

Fig. 5. NCR for SIR model – comparison for different link data rates.

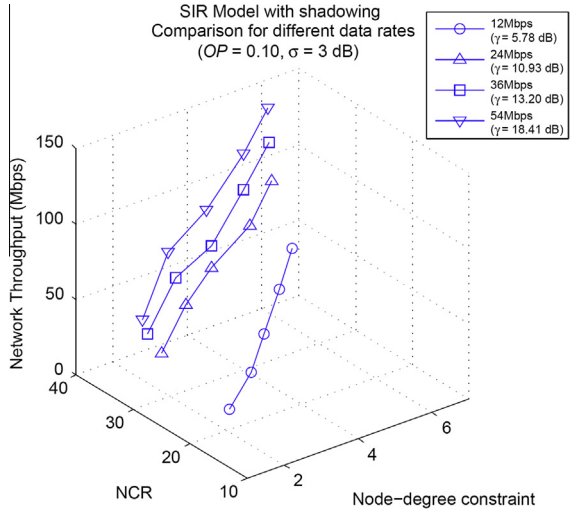

Fig. 6. NCR for SIR model with shadowing – comparison for different link data rates.

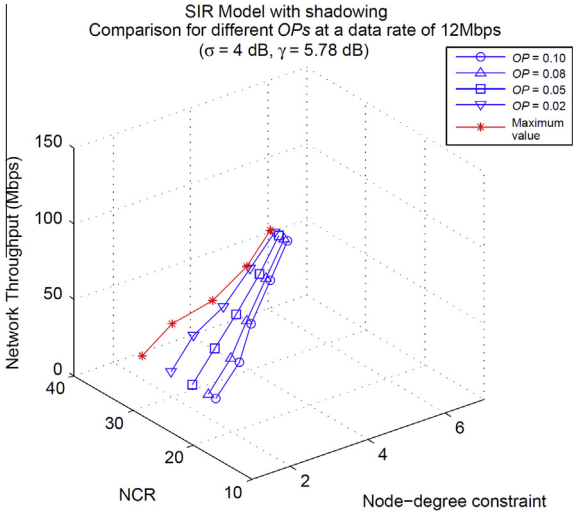

Fig. 8. NCR for SIR model with shadowing – comparison for different *OP*s at a link data rate of 12 Mbps.

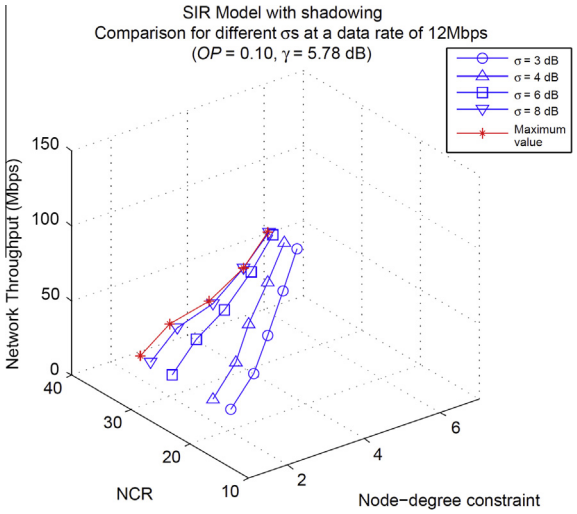

Fig. 7. NCR for SIR model with shadowing – comparison for different σs at a link data rate of 12 Mbps.

models, and has the highest NCR as expected. With the increase in the network throughput with NDC, the NCR increases for all three models. The network throughput depends on the number of links for the GW and increases with an increase in the NDC. Also, the number of links emanating from a mesh node increases with an increase in the NDC. Since the links emanating from a node must be assigned different frequency channels, this increases the NCR.

5.3.2. SIR model

Fig. 5 shows the NCR with SIR model for different data rates. NCR increases with the increase in γ as the data rate increases. An increase in γ means less tolerance for interference in the network. This results in more conflicts in the conflict graph which leads to a higher NCR.

5.3.3. SIR model with shadowing

Figs. 6–8 show the NCR for the SIR model with shadowing for different γ (data rate), σ and *OP*. The NCR for the SIR model with shadowing increases with an increase in γ or σ or with a decrease in *OP*. An increase in σ or a decrease in *OP* translates to an increase in the transmission power of mesh nodes. This causes more interference in the network which results in more conflicts in the conflict graph, thereby leading to a higher NCR.

6. Conclusion

We studied the impact of interference models on channel assignment in MRMC WMNs with the goal of finding a realistic interference-free channel assignment method. We proposed an effective and computationally simple method for constructing the conflict graph using a realistic interference model, i.e. the SIR model with shadowing. We also developed new, simple and effective heuristics for finding WMaISs in the resulting conflict graph. We found that a realistic interference model (the SIR model with shadowing) requires the largest number of frequency channels for interference-free communication in MRMC WMNs when compared to simpler interference models such as the widely-used protocol model. This has important implications for future research in this area.

Further research will mainly focus on finding ways to significantly reduce the number of non-overlapping frequency channels required for the SIR model with shadowing. This paper uses a network of 36 mesh nodes distributed in a 500 m $\times$ 500 m area to evaluate the performance of our channel assignment method. However, our method can be used in a dense deployment of mesh nodes such as occurs in crowded places like train stations and stadiums, and as part of the future work we plan to evaluate the performance of our channel assignment method in such dense mesh networks.

References

[1] P. Gupta, P.R. Kumar, The capacity of wireless networks, IEEE Trans. Inform. Theory 46 (2) (2000) 388–404.
[2] A.U. Chaudhry, N. Ahmad, R.H.M. Hafez, Improving throughput and fairness by improved channel assignment using topology control based on power control for multi-radio multi-channel wireless mesh networks, EURASIP J. Wirel. Commun. Netw. 2012 (2012) 155.
[3] R.M. Karp, Reducibility among combinatorial problems, in: Complexity of Computer Computations, Plenum Press, New York, 1972, pp. 85–103.
[4] A.U. Chaudhry, J.W. Chinneck, R.H.M. Hafez, Channel requirements for interference-free wireless mesh networks to achieve maximum throughput, in: ICCCN, 2013.
[5] M.K. Marina, S.R. Das, A topology control approach for utilizing multiple channels in multi-radio wireless mesh networks, in: Broadnets, 2005.
[6] S. Avallone, I.F. Akyildiz, A channel assignment algorithm for multi-radio wireless mesh networks, Comput. Commun. 31 (7) (2008) 1343–1353.
[7] A. Giannoulis, T. Salonidis, E. Knightly, Congestion control and channel assignment in multi-radio wireless mesh networks, in: IEEE SECON, 2008.
[8] A.P. Subramanian, H. Gupta, S.R. Das, C. Jing, Minimum interference channel assignment in multiradio wireless mesh networks, IEEE Trans. Mob. Comput. 7 (12) (2008) 1459–1473.
[9] A.H.M. Rad, V.W.S. Wong, Cross-layer fair bandwidth sharing for multi-channel wireless mesh networks, IEEE Trans. Wirel. Commun. 7 (9) (2008) 3436–3445.
[10] X.Y. Li, A. Nusairat, Y. Wu, Y. Qi, J.Z. Zhao, X. Chu, Y. Liu, Joint throughput optimization for wireless mesh networks, IEEE Trans. Mob. Comput. 8 (7) (2009) 895–909.
[11] W. Wu, J. Luo, M. Yang, L.T. Yang, Joint interface placement and channel assignment in multi-channel wireless mesh networks, in: IEEE ISPA, 2012.
[12] A. Iyer, C. Rosenberg, A. Karnik, What is the right model for wireless channel interference, IEEE Trans. Wirel. Commun. 8 (5) (2009) 2662–2671.
[13] S. Merlin, N. Vaidya, M. Zorzi, Resource allocation in multi-radio multi-channel multi-hop wireless networks, in: IEEE INFOCOM, 2008.
[14] A. Rajeswaran, G. Kim, R. Negi, Joint power adaptation, scheduling, and routing for ultra wide band networks, IEEE Trans. Wirel. Commun. 6 (5) (2007) 1964–1972.
[15] Y. Xi, E.M. Yeh, Distributed algorithms for spectrum allocation, power control, routing, and congestion control in wireless networks, in: ACM MobiHoc, 2007.
[16] Y. Wang, W. Wang, X.-Y. Li, W.-Z. Song, Interference-aware joint routing and TDMA link scheduling for static wireless networks, IEEE Trans. Parall. Distrib. Syst. 19 (12) (2008) 1709–1726.
[17] M. Alicherry, R. Bhatia, L. Li, Joint channel assignment and routing for throughput optimization in multi-radio wireless mesh networks, in: ACM MobiCom, 2005.
[18] K. Kar, X. Luo, S. Sarkar, Delay guarantees for throughput-optimal wireless link scheduling, in: IEEE INFOCOM, 2009.
[19] B. Wang, G. Zeng, M. Mutka, L. Xiao, Routing for minimum length schedule in multi-channel TDMA based wireless mesh networks, in: IEEE WoWMoM, 2010.
[20] R. Ramanathan, E.L. Lloyd, Scheduling algorithms for multi-hop radio networks, IEEE/ACM Trans. Netw. 1 (2) (1993) 166–177.
[21] T. Rappaport, Wireless Communications: Principles and Practice, second ed., Prentice Hall, Upper Saddle River, NJ, 2002.
[22] N. Nandiraju, D. Nandiraju, L. Santhanam, B. He, J. Wang, D.P. Agrawal, Wireless mesh networks: current challenges and future directions of web-in-the-sky, IEEE Wirel. Commun. Mag. 14 (4) (2007) 79–89.
[23] Y. Xiao, J. Rosdahl, Throughput and delay limits of IEEE 802.11, IEEE Commun. Lett. 6 (8) (2002) 355–357.
[24] R. Fourer, D.M. Gay, B.W. Kernighan, AMPL: A Modeling Language for Mathematical Programming, Duxbury Press, 2002.
[25] IBM ILOG CPLEX. <http://www-01.ibm.com/software/integration/optimization/cplex-optimizer/>.
[26] M.R. Garey, D.S. Johnson, L. Stockmeyer, Some simplified NP-complete graph problems, Theor. Comput. Sci. 1 (1976) 237–267.
[27] S. Avallone, G.D. Stasi, An experimental study of the channel switching cost in multi-radio wireless mesh networks, IEEE Commun. Mag. 51 (9) (2013) 124–134.
[28] W. Si, S. Selvakennedy, A.Y. Zomaya, An overview of channel assignment methods for multi-radio multi-channel wireless mesh networks, J. Parall. Distrib. Comput. 70 (5) (2010) 505–524.
[29] IEEE Standard for IT-Telecom. and Info. Exchange between Systems-Local and Metropolitan Area Networks-Specific Requirements – Part 11: Wireless LAN MAC and PHY Specifications, IEEE Std 802.11, 2007 (Revision of IEEE Std 802.11, 1999).
[30] Richard Van Nee, Ramjee Prasad, OFDM for Wireless Multimedia Communications, Artech House Publishers, 2000.

Aizaz U. Chaudhry received his MASc degree in Electrical and Computer Engineering from Carleton University, Ottawa, Canada, in August 2010, and his BSc degree in Electrical Engineering from University of Engineering and Technology, Lahore, Pakistan, in November 1998. He has several years of professional experience in reputed companies like Philips and Siemens. Currently, Aizaz is a PhD candidate in the Electrical and Computer Engineering program of Carleton University, Ottawa, Canada. He conducts research in the area of wireless mesh networks with focus on interference modeling, topology control, channel assignment and optimization of multi-radio multi-channel wireless mesh networks.

Roshdy H.M. Hafez obtained the Ph.D. in Electrical Engineering from Carleton University, Ottawa, Canada. He joined the Department of Systems and Computer Engineering at Carleton University as an assistant professor, and is now a full professor. Professor Hafez has many years of experience in the areas of wireless communications, RF and spectrum engineering. His current research focuses on broadband wireless networking, 3G/4G, wireless mesh and sensor networks. He acts as a consultant to Industry Canada, CRC, and other telecommunications companies. Between 1994 and 2000, he was actively involved and led projects in federal/provincial centers of excellence: TRIO, CITR and CITO.

John W. Chinneck is a professor in the Department of Systems and Computer Engineering. His degrees are from the University of Waterloo in Systems Design Engineering (BASc 1977, MASc 1978, PhD 1983). Professor Chinneck conducts research in the general area of applied optimization, including various applications in engineering. He is a member of the advisory board and former Editor-in-Chief (2007–2012) of the INFORMS Journal on Computing, a member of the editorial board for the journal Constraints, and a past member of the editorial board for Computational Management Science. He is a past Chair (2005–2007) of the INFORMS Computing Society.